



Local factors contributing to daytime, nighttime, and compound heatwaves in the Eastern mediterranean

Ilias Petrou¹ · Pavlos Kassomenos¹

Received: 28 January 2025 / Accepted: 2 March 2025 / Published online: 11 March 2025
© The Author(s), under exclusive licence to Springer-Verlag GmbH Austria, part of Springer Nature 2025

Abstract

The Eastern Mediterranean region is increasingly experiencing extreme heatwaves, posing significant challenges to public health and ecosystems. Earlier research has categorized heatwaves into three types: independent daytime, independent nighttime, and compound events, and has analyzed their long-term trends. However, the mechanisms driving variations in these different heatwave types are still not well understood. This study investigates the classification and driving mechanisms of heatwave events in the Eastern Mediterranean during the summer period between 1981 and 2023. Using reanalysis datasets, we found a significant increase in the frequency of here examined heatwave types, with compound heatwaves exhibiting the most pronounced amplification in both frequency and intensity. Mechanistic analyses revealed distinct atmospheric and land-atmosphere interactions driving each heatwave type. Daytime heatwaves were linked to hot, dry conditions with high solar radiation, low specific humidity, and reduced cloud cover. Nighttime heatwaves were associated with hot, humid environments characterized by increased cloud cover and longwave radiation, maintaining elevated nighttime temperatures. Compound heatwaves combined mechanisms of both daytime and nighttime heatwaves, exhibiting enhanced solar radiation during the day and increased longwave radiation at night. Spatial variability in these processes highlighted the role of local topographical and land-cover conditions, with regions such as South Italy, West Turkey, Central Greece, and the Adriatic coast showing the strongest trends. Our findings emphasize the influence of anthropogenic climate change on the intensification of heatwaves and the critical role of land-atmosphere interactions in shaping these events. These results highlight the need for region-specific adaptive strategies, including improved urban planning, enhanced vegetation cover, and climate-informed policies, to mitigate the escalating impacts of heatwaves. Further integration of observational data with model simulations is essential to refine forecasts and project future changes in heatwave dynamics.

Keywords Extreme temperature events · Land-atmosphere interactions · Heatwave drivers · Mediterranean climate · Reanalysis datasets

1 Introduction

Heatwaves (HWs) are a natural hazard characterized by temperatures that significantly exceed historical averages for a particular area and time of year. These extreme events

may be accompanied by high/low humidity and limited ventilation, and can have profound impacts on human health, ecosystems, and infrastructure. Their significance lies in their ability to disrupt daily life (Fransson et al. 2023), strain energy and water resources (Zuo et al. 2015), and lead to increased mortality rates (Gasparrini and Armstrong 2011; Arsal et al. 2022; Liu et al. 2024). In recent decades, the frequency, intensity, and duration of heatwaves have been on the rise, largely due to climate change (Perkins et al. 2012). Europe has witnessed a sharp increase in heatwave events over the past few decades (Russo et al. 2015). The European heatwave of 2003 (in July and August) was one of the most intense in recorded history, leading to approximately 70,000 excess deaths, crop failures due to severe drought,

✉ Ilias Petrou
petroui@hotmail.com

Pavlos Kassomenos
pkassom@uoi.gr

¹ Laboratory of Meteorology, Department of Physics, University of Ioannina, University Campus, Ioannina GR- 45110, Greece

and forest fires that ravaged large areas, particularly in Portugal (García-Herrera et al. 2010). In 2010 (in July and August), Eastern Europe and Russia endured a heatwave of unprecedented magnitude and it caused ~ 56,000 heat-related deaths, widespread wildfires and an overall economic toll of \$15 billion, primarily from agricultural losses and firefighting costs (Dole et al. 2011). More recently, the 2018 heatwave (starting in April and lasting until October) affected numerous European countries, breaking temperature records and leading to widespread impacts on the environment, public health, and various sectors of the economy (Hoy et al. 2020). The Mediterranean region is recognized as a climate change hot-spot, experiencing warming at a rate faster than the global average (Lazoglou et al. 2024). Countries in the Eastern Mediterranean have experienced unprecedented heat events in recent years (Zittis et al. 2016). For instance, during the summer of 2021 (July–August), Greece experienced one of the most severe heatwaves in its recent history (Founda et al. 2022). Furthermore, the summer of 2024 was the hottest on record globally, with the Mediterranean region experiencing temperatures significantly above average.

There is no universally accepted definition of HWs in the literature due to the significant attention surrounding HWs as well as the diverse sectors and systems affected by their consequences. Consequently, climatologists have adopted a variety of definitions tailored to the specific goals and concerns of their studies, however they are often focused on the statistical characteristics of unusually rare climatic events (Anderson and Bell 2011; Fischer and Schär 2010). Although HWs are generally recognized as extended periods of extreme heat, the criteria used to define “excess heat” vary widely. These criteria include upper percentiles of air temperature distributions from specific stations (Perkins and Alexander 2013; Russo et al. 2014), as well as fixed absolute thresholds (Meehl and Tebaldi 2004; Nairn and Fawcett 2015). For instance, high temperature extremes typically refer to events where the daily maximum (T_{\max}) or minimum (T_{\min}) temperature surpasses a defined threshold (Su and Dong 2019; Barbier et al. 2017; Schoetter et al. 2015). Definitions based on T_{\max} and T_{\min} are often used to distinguish between daytime and nighttime HWs (Ullah et al. 2019). Unlike heat events that are based solely on T_{\max} and T_{\min} , compound HWs involve the combined impacts of both daytime and nighttime heat extremes (Chen and Zhai 2017). These events are significant because they amplify the impact of HWs and pose unique challenges to human and natural systems (Ridder et al. 2021; Wang et al. 2020a; Zscheischler et al. 2020).

Several studies have explored the physical mechanisms responsible for triggering HWs events in Europe (Carril et al. 2008; Della Marta et al. 2007; Purich et al. 2014). Most

of HWs studies agree that the HWs are primarily driven by atmospheric circulation anomalies and the interaction between soil moisture and air temperature through biophysical processes (Liu et al. 2020a, b). During the summer, Blocking and the Atlantic Low are considered the main circulation patterns that are associated with warm European summer temperatures (Cassou et al. 2005). More specifically, the anticyclonic conditions over Northern Europe, linked to atmospheric blocking, transport air from the east. This air has spent enough time over land to warm up, bringing warmer air, particularly to central and Northern Europe. For instance, the intense European heatwave of August 2003 and the unusually warm conditions of July 2013 were associated with an atmospheric blocking pattern (Black et al. 2004; Vautard et al. 2013). On the other hand, the Atlantic Low exerts its greatest influence on Southern regions. It facilitates the movement of warm air from Northern Africa and the Mediterranean basin toward the north (Cassou et al. 2005). For example, the intense heat of the summer of 2015 in Southern Europe is associated with an Atlantic Low-pressure system (Wehrli et al. 2019).

Though blocking or persistent high-pressure systems are essential synoptic components of HWs, their interaction with the land surface may play an even more critical role. The impact of land surfaces on climate is primarily determined by soil moisture, which regulates how heat fluxes are distributed. In wet soils, evaporation is possible, leading to a high evaporative fraction (the proportion of latent heat flux to net radiation), whereas dry soils are characterized by a dominance of sensible heat flux. Studies on the associations between the land surface and extreme temperatures have found that interactions between soil moisture and temperature amplify summer temperature variability, leading to extreme heat during periods of low soil moisture (Wang et al. 2024; Vogel et al. 2017; Douville et al. 2016). For example, during the 2015 heatwave over the Northern Europe, unusually low soil moisture triggered land-atmosphere feedbacks that limited surface latent heat fluxes, reduced cloud formation, increased surface net radiation, and led to higher temperatures in many European regions (Dirmeyer et al. 2021). Liu et al. (2020b, a), also found that a strong moisture-temperature connection intensified the European HWs of 2003 and 2010. Additionally, it is estimated that during the most recent 2023 heatwave, if the soils had not been dry, the intensity of extreme temperature records would have been reduced by 2.19 °C across Western Mediterranean (Lemus-Canova et al. 2024). Along the same lines, Stéfanon et al. (2014) found that the feedback of soil moisture and temperature, contributed for up to 20% of the extreme temperatures in Eastern France and Western Germany, during the 2003 heatwave. On the other hand, a negative feedback loop can arise when wetter initial

soil conditions promote latent heat flux over sensible heat flux, particularly as temperatures begin to rise during the early summer. Higher temperatures increase latent heat flux, elevating atmospheric humidity, which facilitates cloud formation by lowering the dew point. This leads to reduced net radiation, cooler temperatures, diminished atmospheric demand, and relatively higher soil moisture levels (van Heerwaarden and Teuling 2014).

Moreover, soil moisture can affect precipitation through various mechanisms, with one of the most direct being moisture recycling, where moisture evaporated from the soil contributes to regional precipitation. The impact of soil moisture on precipitation depends largely on two key processes: the proportion of soil moisture that evaporates and the fraction of that evaporation that ultimately falls as precipitation (Wei and Dirmeyer 2012). The impact of precipitation and soil moisture anomalies on the development of HWs has been analyzed across various regions in Europe (Felsche et al. 2024; Vautard et al. 2007). For example, studies based on precipitation anomalies related indices agree that heatwave events in Southern Europe show a degree of sensitivity to dry conditions (Rouges et al. 2023; Hirschi et al. 2011). Other research also shows a strong connection between unusually dry summers in Western and Northern Europe and the frequency of HWs in those areas (Rousi et al. 2022). According to Tripathy and Mishra (2023), during the 2022 European heatwave decreased soil moisture caused by insufficient rainfall and elevated temperatures intensified the drought's persistence and severity, creating a positive feedback loop in which dry soils further exacerbated arid conditions. Nevertheless, some studies mention negative feedbacks mechanisms between soil moisture and precipitation (Yang et al. 2022; Guillod et al. 2015). Taylor (2015) found that the convective precipitation tends to initiate more frequently over dry soils, while Boé (2013) detect a negative soil moisture–precipitation feedback during warm conditions with a Blocking pattern over France.

To date, much of the published literature on HWs has primarily concentrated on a single type of heat event, focusing either on daytime or nighttime temperature extremes (Founda and Giannakopoulos, 2009; Serra et al. 2024; Dong et al. 2018). Only a few recent studies have explored the processes and mechanisms involved in compound HWs, including the previous work of Luo et al. (2022); Wang et al. (2020a) in China, as well as Wu et al. (2023) on a global scale. In Europe, studies on compound events have largely examined the co-occurrence of heat and drought (Tripathy and Mishra 2023; Ionita et al. 2021) or the link between HWs, droughts, and wildfires (Sutanto et al. 2020). However, the processes and mechanisms driving daytime, nighttime, and compound HWs at the European scale remain poorly understood. In particular, there is a lack of research

focusing on the Eastern Mediterranean, a region highly vulnerable to extreme heat events due to its complex climatic and geographical characteristics.

To address this gap, the present study aims to: (1) identify and characterize the key atmospheric mechanisms driving the occurrence of compound HWs, as well as independent daytime and nighttime HWs, in the Eastern Mediterranean; (2) analyze the spatial and temporal distribution of these events using high-resolution hourly reanalysis temperature data; and (3) investigate the associated synoptic patterns and large-scale atmospheric drivers to improve our understanding of the factors influencing extreme heat. A 31-day time window is used to establish temperature thresholds based on long-term T_{\max} and T_{\min} records, ensuring a robust definition of HWs at each grid cell. By providing a comprehensive assessment of these mechanisms, this study contributes to enhancing predictive capabilities for extreme heat events, which is crucial for climate adaptation and risk management strategies in the region.

2 Data and methodology

2.1 Study area

The study area covers Southeastern Europe and the Eastern Mediterranean region, spanning from 30°N to 45°N latitude and 10°E to 35°E longitude (Fig. S1). This region includes parts of southern Europe, the Balkans, Turkey, and the Eastern Mediterranean basin. It is characterized by a diverse topography, including mountain ranges such as the Alps, Carpathians, and Pindus, as well as extensive coastlines along the Adriatic, Aegean, and Eastern Mediterranean seas. The region also features significant inland areas, contributing to its climatic variability.

The climate of the study area can be characterized using the Köppen-Geiger classification, which provides a systematic framework for categorizing climate types based on temperature and precipitation patterns (Peel et al. 2007). Within this classification, the region exhibits considerable climatic diversity, influenced by its complex topography and proximity to large water bodies (Fig. S2). The coastal areas of Greece, Italy, Turkey, and the Eastern Mediterranean predominantly experience a Mediterranean climate, characterized by hot, dry summers and mild, wet winters. In contrast, the northern and inland portions of the Balkans are dominated by temperate oceanic and continental climates, which are marked by higher precipitation levels and colder winter temperatures compared to the Mediterranean zone. Additionally, semi-arid and arid conditions prevail in parts of southern Turkey and inland southeastern Europe, where lower precipitation and greater temperature variability

contribute to distinct climatic conditions. The spatial distribution of these climate types plays a crucial role in shaping atmospheric patterns, particularly in relation to temperature variability and extreme weather events. The combination of maritime influences, mountainous terrain, and continental air masses contributes to the complexity of climatic conditions across the region.

2.2 Data

The data used in the present study consists of atmospheric hourly grid point values for the Southeastern Europe (Eastern Mediterranean) region with a $0.25^\circ \times 0.25^\circ$ spatial resolution ($30\text{--}45^\circ\text{N}$ and $10\text{--}35^\circ\text{E}$, Fig. S1). More specifically, hourly 2-meter air temperature (K) over the past 42 years (1981–2023) in summer (June–August) were obtained from the fifth generation ERA5 data set of by the European Centre for Medium-Range Weather Forecasts (<https://cds.climate.copernicus.eu/datasets/reanalysis-era5-single-levels?tab=overview>). To detect daytime, nighttime and compound HWs, daily maximum 2-meter (T_{\max}) and daily minimum 2-meter air temperature (T_{\min}) were used from the temperature dataset above. Hourly ERA5 reanalysis of other atmospheric variables, including 2-meter specific humidity (g/kg), total cloud cover (%), total precipitation (mm), latent and sensible surface fluxes (W/m^2), soil moisture (0–7 cm) (m^3/m^3) and surface radiation (W/m^2) for 1981–2023 at a spatial resolution of $0.25^\circ \times 0.25^\circ$ were also used, to explore the local mechanisms and processes associated with each type of HWs in Eastern Mediterranean. While the ERA5 reanalysis dataset provides a high temporal resolution and is valuable for understanding long-term atmospheric trends, it does have some limitations. The spatial resolution of $0.25^\circ \times 0.25^\circ$ may not fully capture finer-scale atmospheric phenomena or localized processes, particularly in complex or heterogeneous terrains such as mountainous regions. Additionally, uncertainties in model-based reanalysis products, such as biases in the representation of small-scale convective processes or local weather phenomena, may affect the accuracy of some variables, especially for extreme events. These limitations should be considered when interpreting the results, especially in regions with highly variable local conditions.

2.3 Independent and compound heatwave detection

Several methods and approaches have been proposed to define HWs, and they can vary based on geographical context, climate conditions, and the specific impact being measured. Temperature is a fundamental factor in defining HWs and one commonly recognized approach is based on

the historical temperature records for a specific area. For instance, a heatwave can be identified when temperatures exceed a certain percentile (e.g., the 90th or 95th percentile) of historical data for a certain location (Su and Dong 2019; Luo et al. 2022; Wu et al. 2023). In this study, here examined types of HWs were defined based on summer daily T_{\max} and T_{\min} , as well as on the 90th percentiles of summer daily T_{\max} and T_{\min} temperatures ($C_{90\max}$ and $C_{90\min}$ respectively) during the reference period of 1981–2010. To determine the $C_{90\max}$ and $C_{90\min}$ for each grid point, a 31-day window (fifteen days before and after) was created for each calendar day of the year over the reference period (1981–2010). For each 31-day window, the 90th percentile of daily T_{\max} and T_{\min} temperatures was calculated and this process repeated for each day of the year, sliding the 31-day window along by one day. Subsequently, the $C_{90\max}$ and $C_{90\min}$ percentiles served as the hot thresholds for identifying HWs. More specifically, independent daytime HWs (DHW) are identified if only T_{\max} exceeds its 90th percentile, but T_{\min} does not ($T_{\max} > C_{90\max}$ and $T_{\min} < C_{90\min}$), independent nighttime HWs (NHW) are identified if only T_{\min} exceeds its 90th percentile, but T_{\max} does not ($T_{\max} < C_{90\max}$ and $T_{\min} > C_{90\min}$), and compound HWs (CHW) when both T_{\max} and T_{\min} exceed their respective 90th percentiles ($T_{\max} > C_{90\max}$ and $T_{\min} > C_{90\min}$) during 1981–2023 (Luo et al. 2022; Thomas et al. 2020). According to previous studies, a heatwave must persist for at least three consecutive days to qualify as a heatwave event (Perkins and Alexander 2013; Russo et al. 2014). If a sequence of heatwave days is shorter than three days, it does not qualify as a heatwave (Fig. S3). Therefore, a temporal filter for persistence was applied to check for sequences of heatwave days (consecutive days fulfilling the heatwave condition).

A key advantage of this approach is the explicit consideration of NHW, which are often overlooked in definitions that rely exclusively on daytime temperature thresholds. NHW can have significant consequences for human health, energy demand, and ecosystems, particularly in urban areas where nighttime cooling is limited. Additionally, this methodology identifies CHW, where both T_{\max} and T_{\min} exceed their respective 90th percentiles, capturing events that are potentially more impactful than those characterized by daytime extremes alone. Furthermore, the use of a sliding 31-day window for percentile calculations ensures that thresholds are dynamically adjusted to seasonal variations, providing a more accurate representation of extreme temperature events. This approach enhances the regional applicability of this analysis, particularly in a climatically diverse area such as the Eastern Mediterranean, where local-scale factors influence temperature extremes.

To provide a multidimensional view of here examined types of HWs and fully understand their effects on annual

basis, we utilized three metrics including: the annual frequency of HWs (HWF), the annual mean intensity of HWs (HWI), and the annual cumulative intensity of HWs (HWCI) (Wu et al. 2023; Ji and Chen 2024; Li et al. 2017). The HWI measures how extreme the heatwave is during the event by quantifying how much hotter the temperature was compared to the climatological threshold (90th percentile) for a particular grid point and day. Since independent DHW are characterized by T_{max} exceeding its threshold, the daily HWI (HWI_{daily}) for DHW is calculated as:

$$HWI_{daily}^{DHW} = (T_{max} - C_{90max})_{\geq 3day} \quad (1)$$

However, to properly account for the nighttime contribution in NHW and CHW events, we adapted the HWI metric accordingly. For NHW, where T_{min} exceeds its threshold but T_{max} does not, the HWI is calculated as:

$$HWI_{daily}^{NHW} = (T_{min} - C_{90min})_{\geq 3day} \quad (2)$$

For CHW, where both T_{max} and T_{min} exceed their respective thresholds, we define HWI as the total excess heat contribution from both variables:

$$HWI_{daily}^{CHW} = (T_{max} - C_{90max}) + (T_{min} - C_{90min})_{\geq 3day} \quad (3)$$

This approach ensures that the intensity metric fully captures the excess heat contribution for each type of HW, particularly for NHW and CHW, where nighttime temperatures play a critical role. The HWF measures how often HWs occur over a year and represents the total number of heatwave days ($HWI_{daily} > 0$) within a year. The HWCI measures the total intensity of here examined HWs that occurred during a year. It sums up the daily intensities over all heatwave days within a year and provides a sense of the overall burden or total excess heat experienced during HWs in a given year.

2.4 Analyzing anomalies on the differences between CHW and DHW/NHW

To better understand the relative evolution of CHW compared to DHW and NHW HWs over the last few decades, we examined the anomalies in HWF, HWI, and HWCI. This way we can capture how CHWs are diverging from other heatwave types, providing insights into the changing nature of heatwave events. The differences (Δ) express the relative changes between these heatwave types. The formula for anomalies can be described as follows:

$$\Delta a_{anom} = (a_{CHW} - a_{DHW/NHW}) - (\overline{a_{CHW}} - \overline{a_{DHW/NHW}}) \quad (4)$$

Where a is the heatwave metric (HWF, HWI, HWCI), a_{CHW} is the metric value for CHWs, $a_{DHW/NHW}$ is the corresponding value for DHW or NHW, and $(a_{CHW} - a_{DHW/NHW})$ is the long-term average difference over the whole study period (1981–2023). In this context, the Anomaly of Heatwave Frequency Differences (Δ HWF) was calculated which represents how the HWF of CHW deviates from that of DHW or NHW relative to the long-term mean. In addition, the Anomaly of Heatwave Intensity Differences (Δ HWI) and the Anomaly of Cumulative Heatwave Intensity Differences (Δ HWCI) were quantified, showing how the HWI and HWCI respectively of CHW differs from that of DHW and NHW, compared to the long-term average difference.

2.5 Composite analysis

To identify the prevailing patterns of various atmospheric variables associated with each type of atmospheric heatwave, we employed composite analysis to examine local variables linked to the synoptic patterns of DHW, NHW, and CHW heatwaves. Our approach follows the methodology used by Luo et al. (2022) in analyzing heatwave mechanisms over Southern China. First, the daytime and nighttime averages for each grid point were calculated by averaging the hourly variables during daytime hours (11:00–17:00) and nighttime hours (23:00–05:00), respectively. A 30-year reference period (1981–2010) was used as the climatological baseline for each variable. For each grid point and each day of the year, the long-term daily average (climatology) was computed over this period. To smooth short-term fluctuations and maintain a continuous seasonal cycle, a 31-day rolling average was applied to the daily climatology. The daytime and nighttime anomalies were then determined by subtracting the climatological baseline from the original data, highlighting deviations from the long-term mean during heatwave days.

This process was repeated for each grid point and variable, producing a comprehensive spatial and temporal anomaly map. To construct the composite daytime and nighttime anomalies for each heatwave type, we averaged the mean anomalies across here examined heatwave events of that type, ensuring equal weighting so that no single event disproportionately influenced the composite. The statistical significance of these anomalies was then assessed using the Mann-Kendall test to detect trends, while Sen's slope was used to estimate the magnitude of these trends (Gilbert 1987). By following this approach, consistent with Luo et al. (2022), we ensure methodological rigor in analyzing the atmospheric mechanisms contributing to heatwaves.

3 Results and discussion

3.1 Temporal changes and Spatial distribution of independent and compound heatwaves

For the period between 1981 and 2023, regional summertime DHW, NHW and CHW HWs were determined based on T_{\max} and T_{\min} series in Eastern Mediterranean. Furthermore, to evaluate the variations in the occurrence and severity of different types of HWs for the study period, three key annual metrics were examined: heatwave frequency (HWF), heatwave intensity (HWI) and cumulative heatwave intensity (HWCI), as well as the anomaly trends of the difference (Δ) between CHW and DHW/NHW. Figure 1 demonstrates the time series of the annual mean frequencies of here examined types of HWs. It is apparent that the occurrence frequencies of here examined types of HWs in Eastern Mediterranean have increased over the past 42 years. In addition, the analysis indicates that CHW has consistently shown higher average values and greater variability across all three metrics when compared to DHW and NHW. More specifically, considering the frequency of occurrence, the upward trends are even more pronounced for CHW, where the linear slope reaches 2.91 days/decade, 4 times higher than NHW (0.72 days/decade) and 8.55 higher than DHW (0.34 days/decade). The growth rate of NHW is twice as high as that of DHW (Fig. 1). Recent research has also highlighted that

heat extremes are rapidly becoming more prevalent during nighttime hours (Wang et al. 2020b). This increasing trend of CHW in HWF has affected almost the whole study area, with the most extensive rises occurring in Mediterranean and South Italy (Fig. S4a). Simultaneously, Δ HWF shows a linear increase of 3.16 days per decade for CHW compared to DHW and 2.74 days per decade relative to NHW, as depicted in Fig. 2.

In terms of intensity (HWI), CHW and DHW demonstrates a significant upward trend of 0.02 °C per decade, outpacing the trends observed for NHW, which shows zero increase (Fig. 3). Prolonged daytime heat, combined with minimal nighttime cooling, poses a serious risk, as it can result in heat-related fatalities, especially among individuals with cardiovascular conditions (Majeed and Floras 2022). Notably, the spatial distribution of CHW in HWI differs markedly compared to HWF. The most notable increases in HWI are predominantly located in West Turkey, Italy and regions along the coast of the Adriatic Sea (Fig. S4b). In the meantime, the Δ HWI for CHW compared to DHW and NHW show upward trends, with rates of 0.10 and 0.01 °C per decade, respectively (Fig. 4).

The analysis of HWCI reveals a significant linear increase in CHW, with a trend of 0.44 °C per decade, substantially outpacing the trends observed for DHW (0.09 °C per decade) and NHW (0.04 °C per decade) (Fig. 5). The Δ HWCI trends relative to DHW and NHW show also

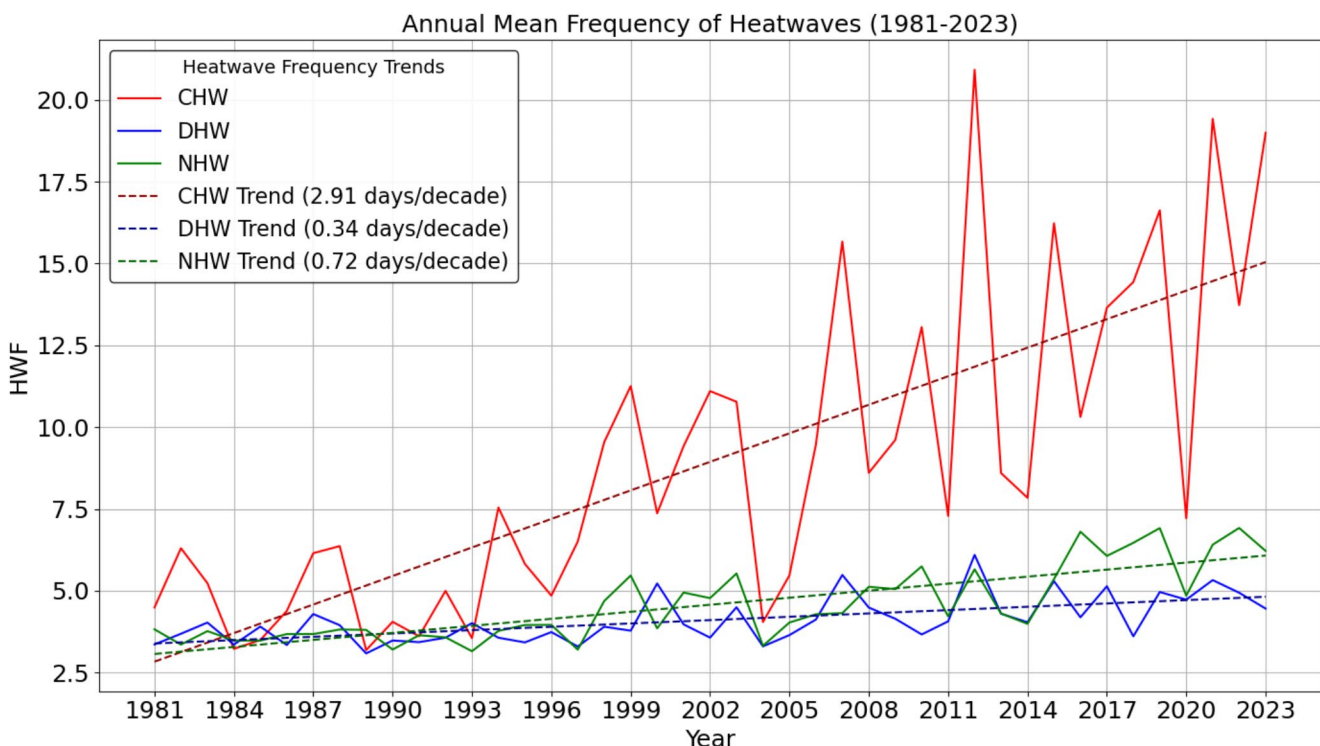


Fig. 1 Time series of the annual mean frequency (HWF) trends of CHW (red), DHW (blue), and NHW (green) from 1981 to 2023. The straight line represents the trend determined by the Mann-Kendall test, with all trends being statistically significant at the 0.05 level

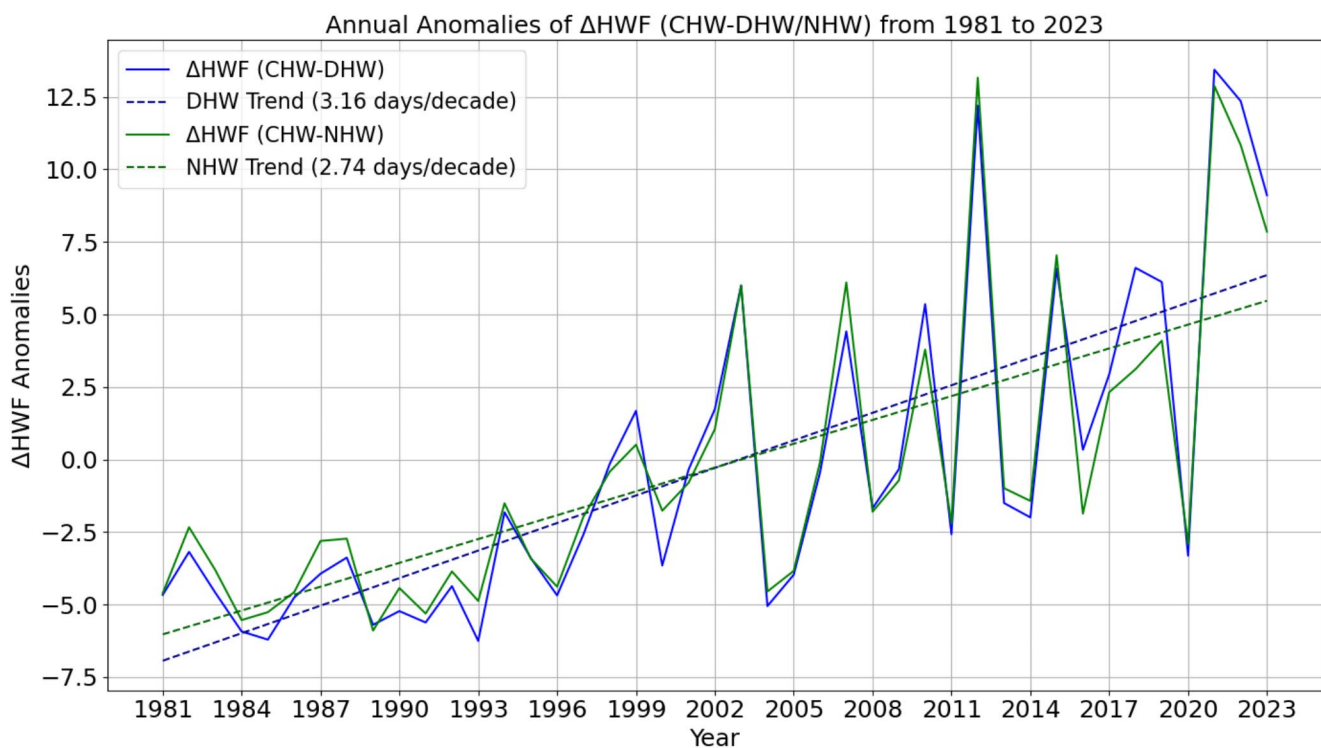


Fig. 2 Time series of the annual anomalies of differences between CHW and DHW/NHW (blue/green) in the metric of frequency (ΔHWF). The straight line represents the trend determined by the Mann-Kendall test, with all trends being statistically significant at the 0.05 level

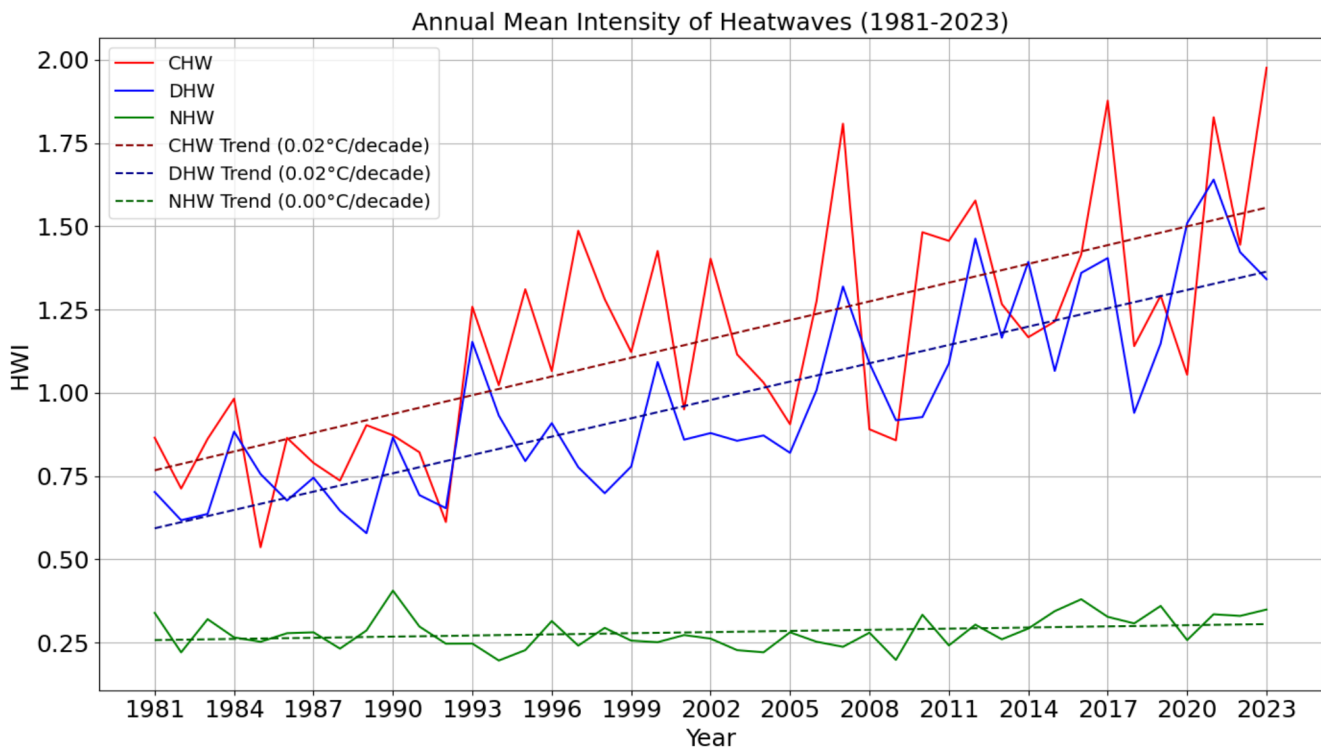


Fig. 3 Time series of the annual mean intensity (HWI) trends of CHW (red), DHW (blue), and NHW (green) from 1981 to 2023. The straight line represents the trend determined by the Mann-Kendall test, with all trends being statistically significant at the 0.05 level

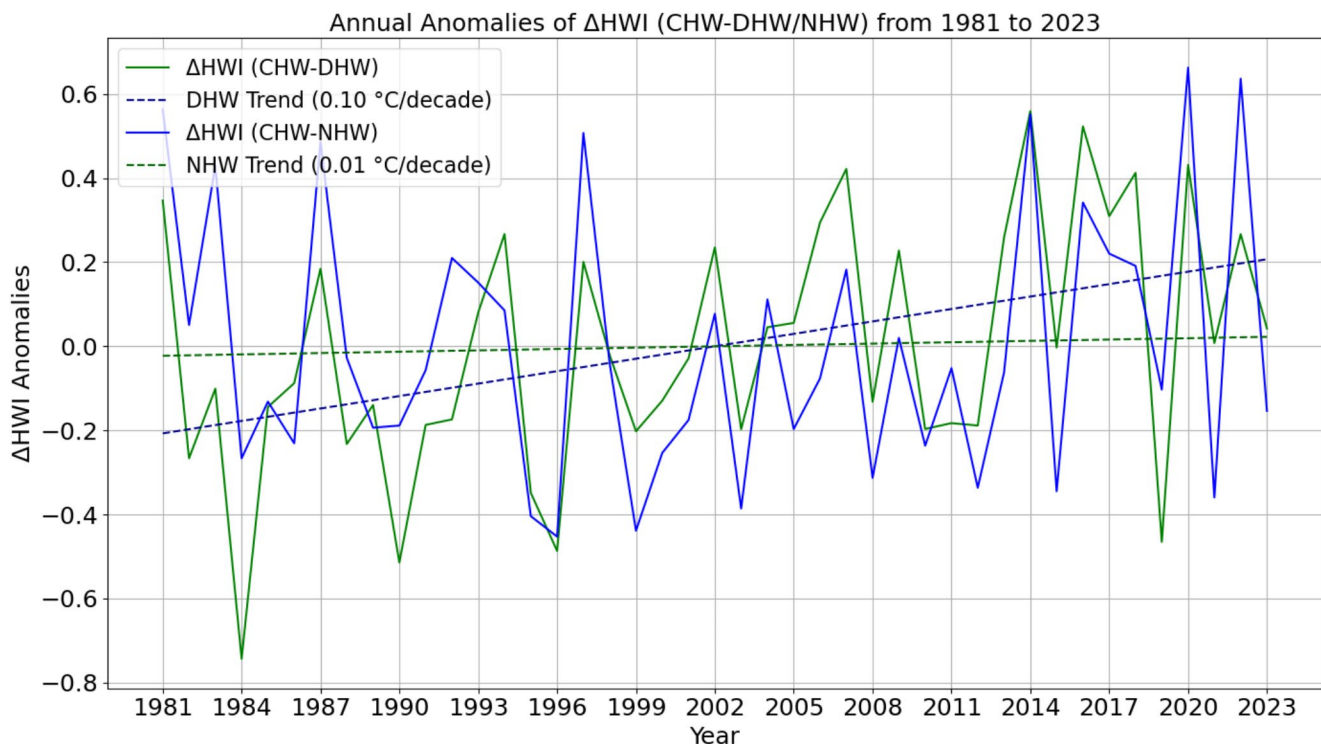


Fig. 4 Time series of the annual anomalies of differences between CHW and DHW/NHW (green/blue) in the metric of intensity (ΔHWI). The straight line represents the trend determined by the Mann-Kendall test, with all trends being statistically significant at the 0.05 level

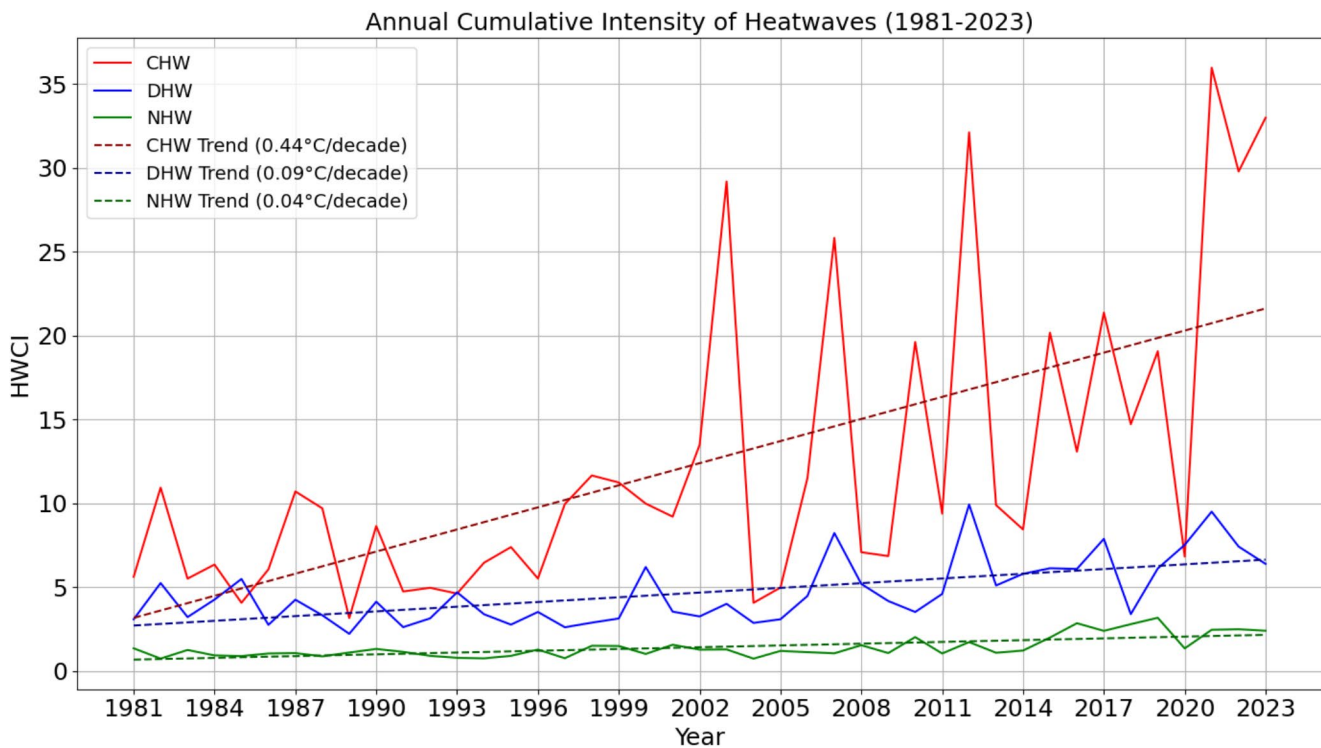


Fig. 5 Time series of the annual mean cumulative intensity (HWCI) trends of CHW (red), DHW (blue), and NHW (green) from 1981 to 2023. The straight line represents the trend determined by the Mann-Kendall test, with all trends being statistically significant at the 0.05 level

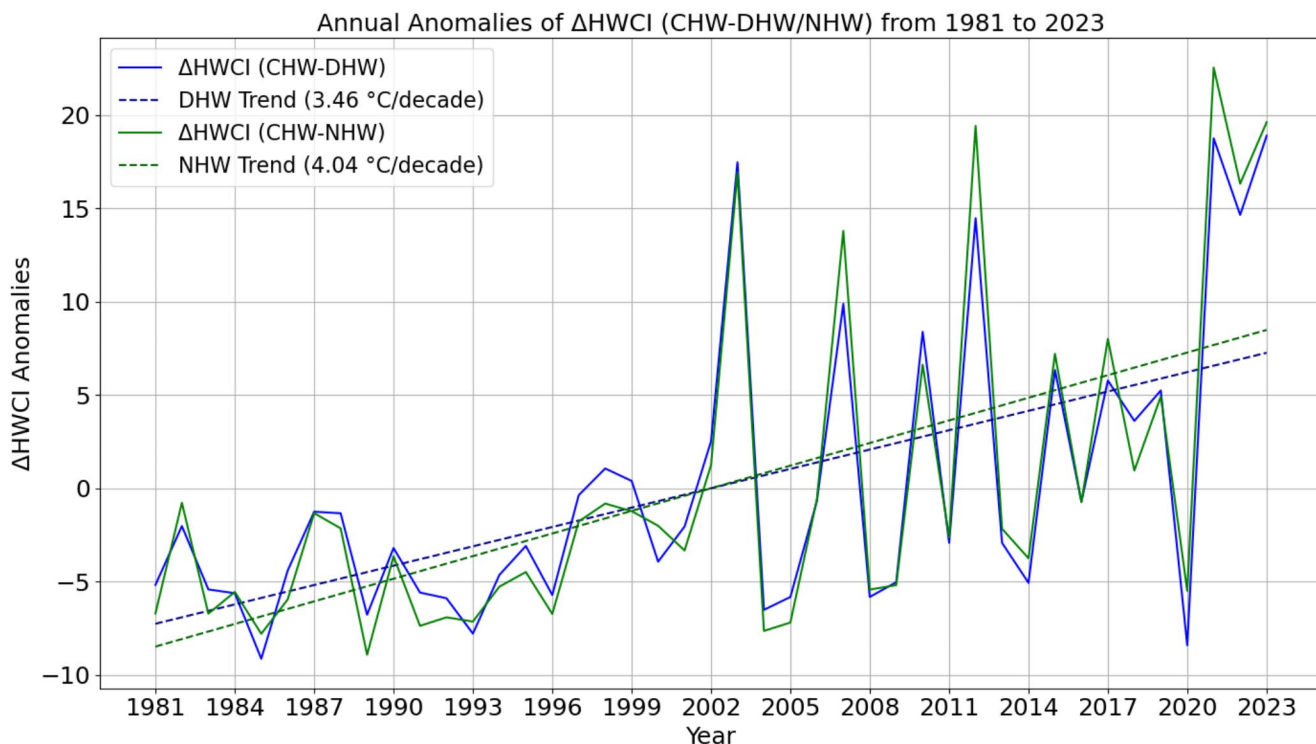


Fig. 6 Time series of the annual anomalies of differences between CHW and DHW/NHW (blue/green) in the metric of cumulative intensity (ΔHWCI). The straight line represents the trend determined by the Mann-Kendall test, with all trends being statistically significant at the 0.05 level

Table 1 Trends in HWF, HWI, and HWCI for each heatwave type (CHW, DHW, NHW) and the anomaly trends (Δ) of CHW relative to DHW and NHW in the Eastern mediterranean during 1981–2023

Metric	CHW Trend	DHW Trend	NHW Trend	ΔCHW vs. DHW	ΔCHW vs. NHW
HWF (days/decade)	+2.91	+0.34	+0.72	+3.16	+2.74
HWI (°C/decade)	+0.02	+0.02	0.00	+0.10	+0.01
HWCI (°C/decade)	+0.44	+0.09	+0.04	+3.46	+4.04

notable linear increasing trends, with magnitudes of 3.46 and 4.04 °C per decade, respectively (Fig. 6). The Mediterranean Sea regions, South Italy, Central Greece, East Turkey and coastal areas of the Adriatic Sea have experienced the most notable growth rates of HWCI (Fig. S4c). These results do not come as a surprise, as the Mediterranean region is one of the areas experiencing the most significant increases in summer temperature extremes worldwide (Pastor et al. 2024). Additionally, in recent decades the frequency of atmospheric HWs has steadily risen, with a notable acceleration in the past twenty years across Southern Europe (Pardo and Paredes-Fortuny 2024) and Northern Africa (Engdaw et al. 2022). Table 1 presents a summary of the key trends in HWF, HWI and HWCI for CHW, DHW, and NHW.

While the role of natural climate variability cannot be excluded, the substantial trends in these metrics strongly suggest that anthropogenic climate change is playing a

significant role in increasing HW occurrence and intensity. The rapid warming in the Eastern Mediterranean aligns with previous research highlighting the role of greenhouse gas emissions, urbanization, and land-use changes (Di Napoli et al. 2018; Oliveira et al. 2022). A key factor in this phenomenon is the Urban Heat Island (UHI) effect, where urban areas experience higher temperatures than their rural counterparts due to the absorption and retention of heat by impervious surfaces, such as asphalt and concrete. These materials absorb significant amounts of solar energy during the day and release it gradually at night, creating warmer nighttime conditions—often exacerbating NHWs. Notably, the greater increase in NHW compared to DHW suggests that longwave radiative effects play a significant role, particularly in urbanized regions where heat retention is amplified by the UHI. Studies on UHI effects, such as those by Lopes et al. (2013) and Oliveira et al. (2021), have shown that urban regions like Lisbon experience distinct changes in thermal patterns due to the UHI effect, which could explain the observed trends in NHWs. These studies confirm that urban areas amplify nighttime warming, especially during heatwaves, by retaining heat in buildings, roads, and other surfaces. Consequently, UHI may act as amplifiers of anthropogenic heatwaves, particularly during the night when radiative cooling is reduced. The increasing urbanization in Mediterranean regions could thus play a critical role

in the observed increase in CHWs, with large metropolitan areas disproportionately contributing to this trend.

3.2 Possible local mechanisms for atmospheric heatwaves

To gain deeper insights into the physical mechanisms driving various types of HWs, composite analysis was employed to investigate variations in several atmospheric variables during heatwave events, including 2-meter temperature, total precipitation, specific humidity, total cloud cover, soil moisture, surface radiation and heat fluxes. At first, Fig. 7 presents composite maps of anomalous near-surface air temperature at 2 m above the ground (T2m) for DHW, NHW, and CHW events occurring in Eastern Mediterranean. It is apparent that during HWs in Eastern Mediterranean, positive T2m anomalies are recorded across a wide region encompassing the entire study area. This suggests that the spatial extent of these events is significantly larger than that of study area, indicating that these HWs are regional in nature, affecting vast areas rather than being confined to localized regions. More specifically, the maps reveal that positive daytime T2m anomalies during DHW (Fig. 7a) are more pronounced than those during daytime hours of NHW (Fig. 7b). Conversely, positive nighttime T2m anomalies during NHW (Fig. 7e) slightly surpass those observed during nighttime hours of DHW (Fig. 7d). As anticipated, CHW (Fig. 7c, f) exhibit the strongest (and over a broader range on a regional scale) positive T2m anomalies across all time periods compared to DHW (Fig. 7a, d) or NHW (Fig. 7b, e).

To explore the mechanisms underlying here examined types of HWs in greater detail, the following discussion will concentrate on the associated patterns of cloud cover, humidity and of downward surface shortwave and longwave radiation. Figure 8 presents the daytime composite anomalies of total cloud cover and specific humidity for here examined types of HWs in Eastern Mediterranean. It's worth mentioning that the nighttime composite anomalies (representing mean values for nighttime hours) for here examined types heatwave types are identical to their respective daytime composites (representing daytime hours) and are therefore omitted from the figures. It is evident that DHW are linked to negative anomalies in daytime cloud cover across the majority of continental regions (Fig. 8a). The reduction in daytime cloud cover allows more solar shortwave radiation to reach the surface (Fig. 9a), leading to an increase in near-surface temperatures (Fig. 7a), as well as the occurrence of DHW. The same pattern is repeated during the CHW (Figs. 7c and 9c). Negative anomalies in daytime specific humidity are also noted mainly across continental regions during DHW (Fig. 8d), which in turn intensifies solar radiation, contributing to the warming of air near the

surface. Negative specific humidity anomalies during DHW (Fig. 8d) indicate dry conditions, which reduce evaporative cooling and amplify warming. In contrast, NHW is associated with positive humidity anomalies (Fig. 8e), likely due to increased moisture retention and cloud formation, which enhance nighttime heat retention (Fernandes and Fragoso 2021).

From another perspective, reduced cloud cover at night results in increased release of longwave radiation directly from the surface. This leads to cooler nighttime temperatures (radiative cooling), maintaining the high temperature anomalies occurring during the day, defining what is known as a daytime heat event. Similar to the case of DHW, CHW are also associated with negative anomalies of daytime cloud cover over almost the entire study area except for the marine areas around South Italy (Fig. 8c) and negative (and zero) anomalies of daytime specific humidity in most continental regions, though covering a smaller spatial extent. During the daytime hours of NHW, positive anomalies of cloud cover are observed over Central-Southern Greece, South Italy and Western Turkey (Fig. 8b) and positive humidity anomalies are present across most of the study area, including continental and marine regions (Fig. 8e). The increased cloud cover reduces the amount of solar radiation reaching the surface (Fig. 9b), resulting in cooler daytime temperatures during NHW compared to DHW (Fig. 7b).

Closer examination of Fig. 9 reveals that during NHW, positive surface downward solar radiation anomalies are substantially weaker compared to DHW, whereas in many areas such as South Greece, East Mediterranean and West Turkey negative anomalies are dominant (Fig. 9b). On the other hand, during NHW, for all regions of the study area, positive downward longwave radiation anomalies were found (Fig. 9e), primarily due to increased cloud cover and atmospheric moisture, since clouds and atmosphere emit more downward longwave radiation toward the surface, which diminishes longwave radiative cooling. This suggests that the elevated temperatures during NHW are likely influenced by alternative heating mechanisms, such as longwave radiative heating. Increased downward longwave radiation during NHW (Fig. 9e) suggests anthropogenic contributions, particularly in urbanized areas where heat is absorbed by buildings and slowly released at night (Oliveira et al. 2021). This aligns with the UHI effect, which amplifies nighttime warming by limiting radiative cooling due to the thermal properties of urban surfaces (Lopes et al. 2013). The intensification of NHW poses serious health and well-being risks, particularly because NHWs disrupt recovery from daytime heat exposure (Di Napoli et al. 2018). The inability to cool down at night disrupts the body's natural recovery processes and can lead to prolonged heat exposure, increasing the risk of heat-related illnesses such as heat exhaustion

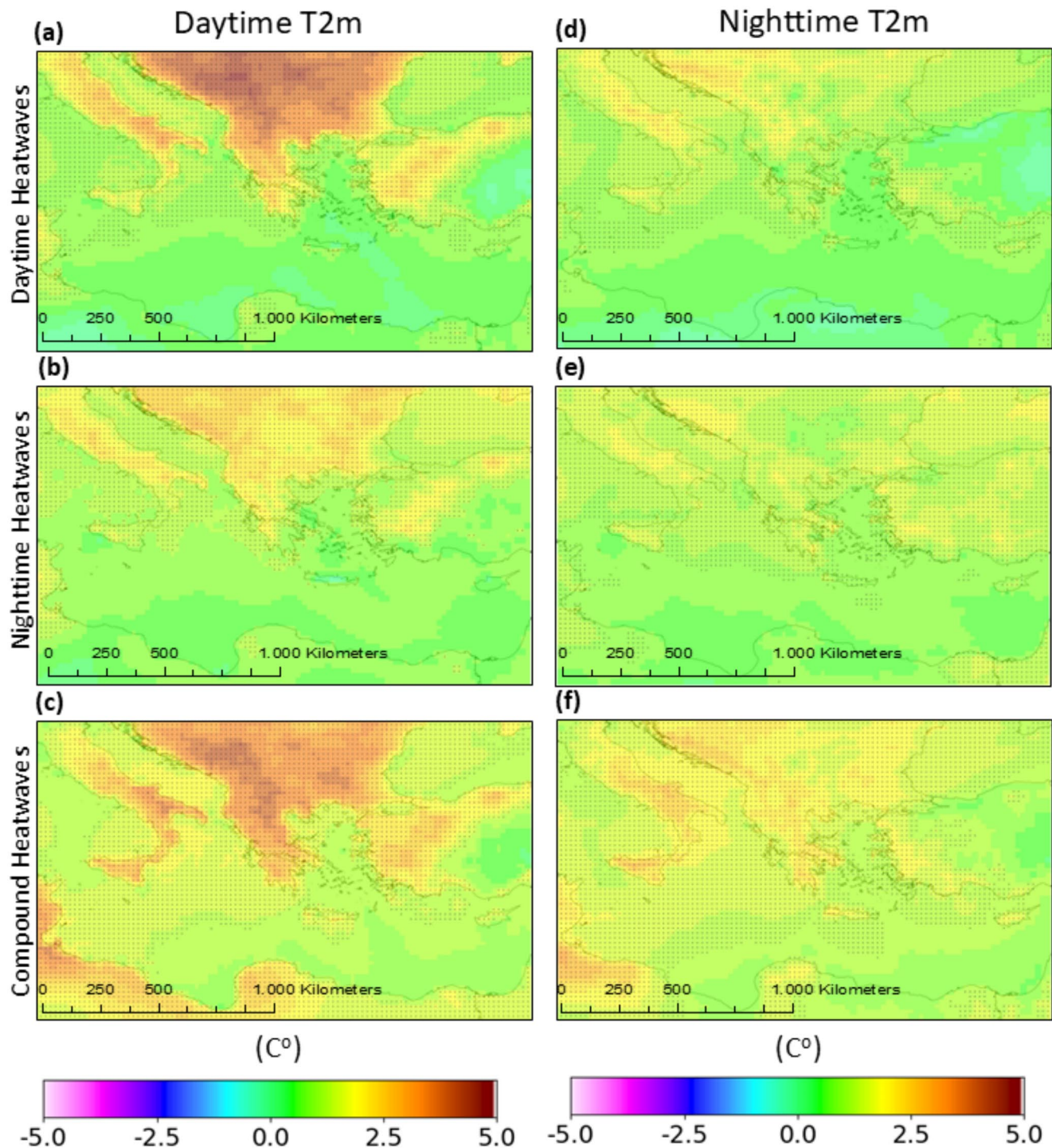


Fig. 7 The daytime (left pannel) and nighttime (right pannel) composite averages of the near-surface temperature (T2m) anomalies for daytime, nighttime, and compound HWs in Eastern Mediterranean. Dots indicate statistical significance at the 0.05 level, determined using

Mann-Kendall test. The daytime (nighttime) composites are derived from data recorded during daytime (nighttime) hours throughout the heatwave events

and heat stroke. Vulnerable populations, such as elderly individuals, those with pre-existing health conditions, and lower-income groups without access to cooling systems, are at increased risk of heat stress and sleep disturbances. The

rising frequency of NHW events underscores the need for urban adaptation measures, such as increased vegetation, reflective materials, and better building insulation, to mitigate the impacts of nighttime heatwaves on public health.

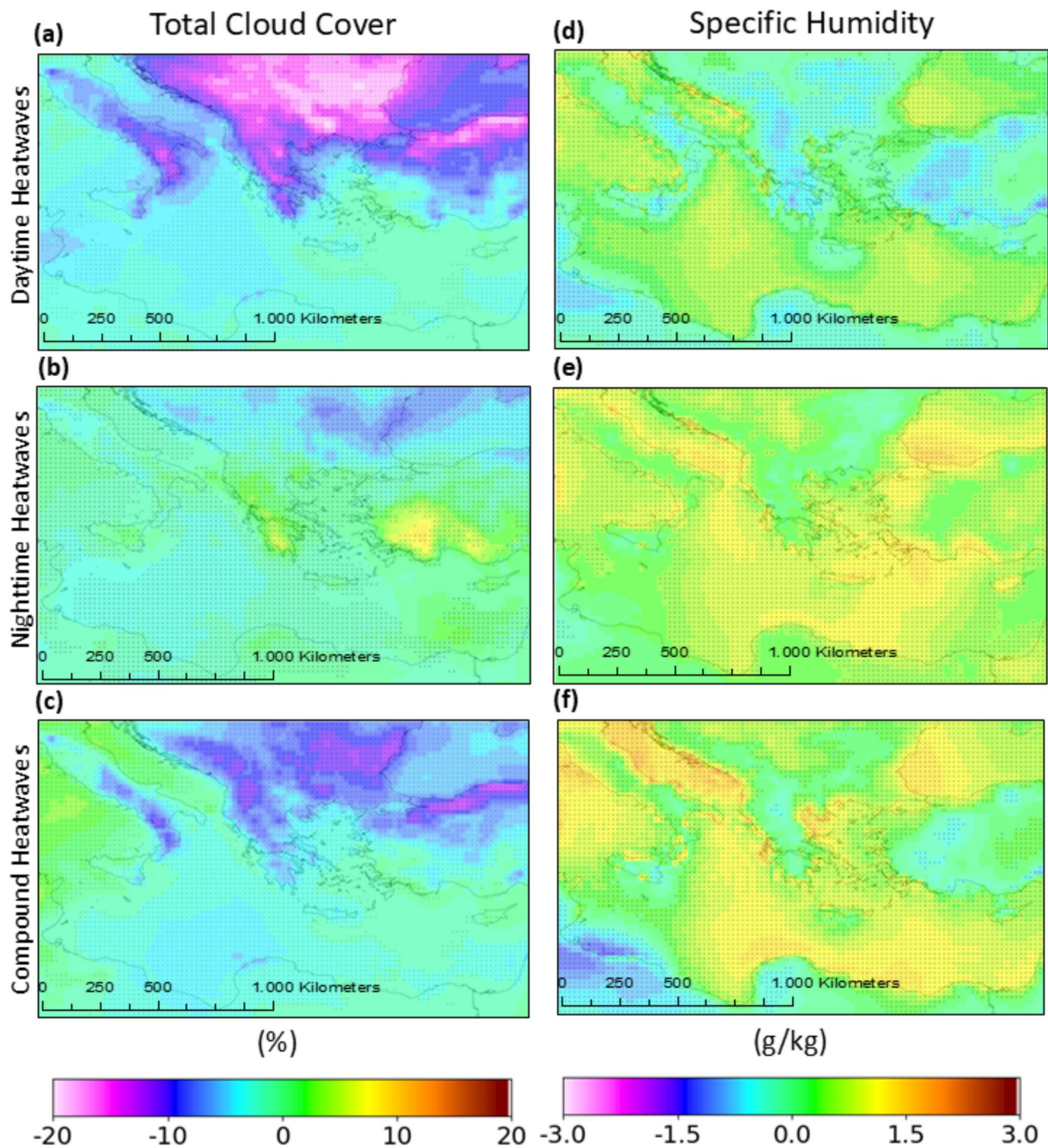


Fig. 8 The daytime composite averages of the total cloud cover anomalies (left pannel) and near-surface specific humidity (right pannel) for daytime, nighttime, and compound HWs in Eastern Mediterranean.

Dots indicate statistical significance at the 0.05 level, determined using Mann-Kendall test

Additionally, as shown in Fig. 9d, DHW are associated with positive downward longwave radiation anomalies in many areas, as well as with negative and zero values of downward longwave radiation anomalies, indicating increased longwave radiative cooling driven by a reduction in cloud cover.

Regarding CHW, a combination of enhanced solar radiation during the day (Fig. 9c), compared to NHW, and weaker longwave radiative cooling at night (Fig. 9f), relative to DHW, contribute to unusually high temperatures throughout both day and night (Fig S5).

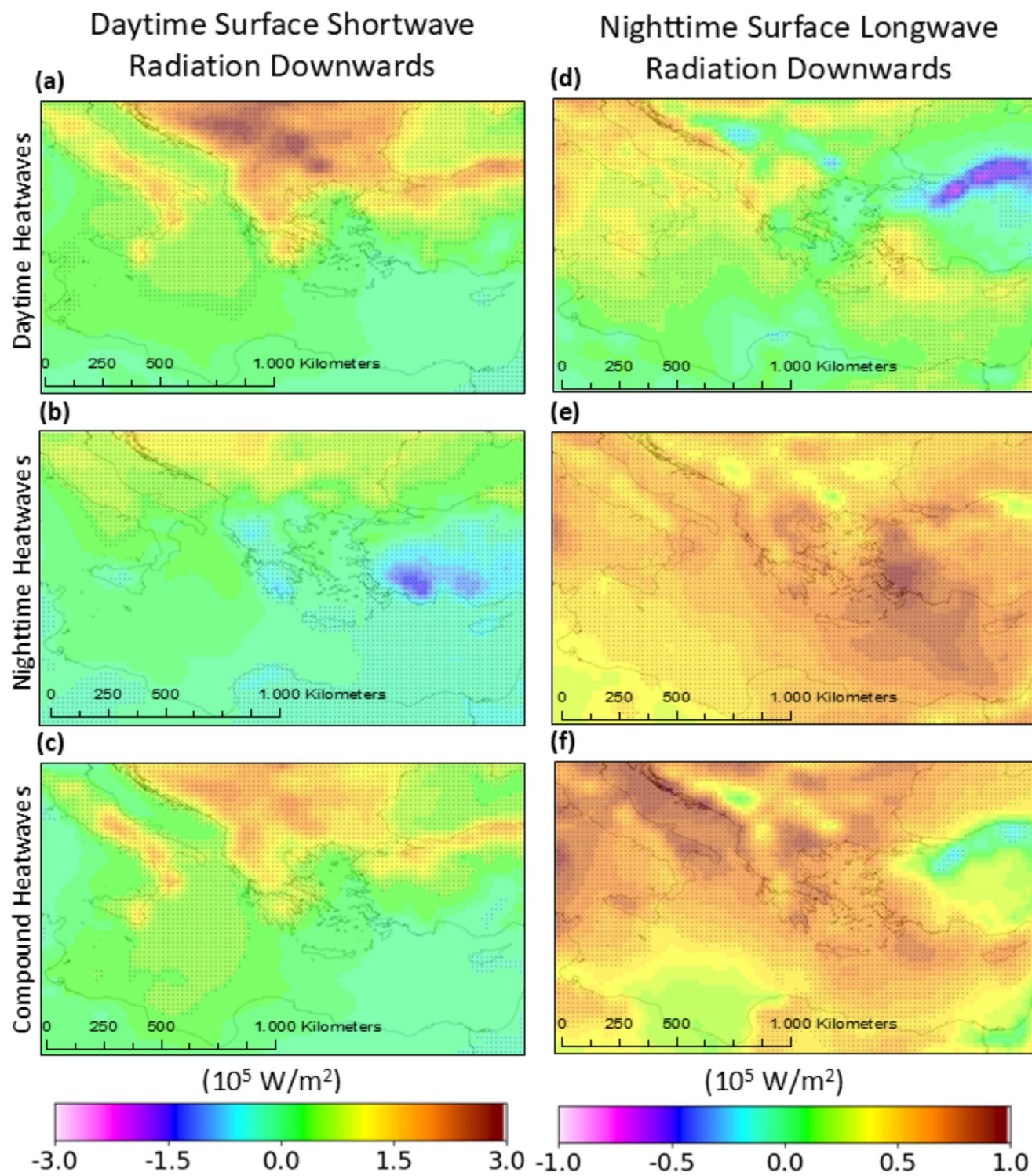


Fig. 9 The composite averages of the daytime surface shortwave radiation downwards anomalies (left pannel) and nighttime surface longwave radiation downwards anomalies (right pannel) for daytime,

nighttime, and compound HWs in Eastern Mediterranean. Dots indicate statistical significance at the 0.05 level, determined using Mann-Kendall test

Soil moisture also plays a critical role in modulating HWs due to their role in the surface energy balance, evapotranspiration, and atmospheric feedback mechanisms, particularly in regions like the Mediterranean, where land-atmosphere interactions are strong (Felsche et al. 2023; Lemus-Canovas et al. 2023). Additionally, soil moisture influences how the available surface energy is distributed between sensible heat flux and latent heat flux. The composite of daily total precipitation and near surface soil moisture (0–7 cm) anomalies during the DHW, NHW and CHW events are shown in Fig. 10. Clearly, the DHW and CHW are associated with negative anomalies in precipitation (Fig. 10a, c) and soil moisture (Fig. 10d, f) over most of the continental regions, showing positive anomalies over Central Turkey. The depletion of soil moisture weakens evaporative cooling, enhancing surface heating and intensifying HWs. Additionally, soil moisture deficits create positive feedback loops that prolong heatwave conditions, suppress cloud formation, and reduce precipitation (Lemus-Canovas et al. 2023). Conversely, NHWs exhibit weaker negative precipitation and soil moisture anomalies, with positive anomalies observed not only in Turkey but also in South Greece and South Italy (Fig. 10b, f).

The alterations in soil moisture and precipitation were associated with changes in latent and sensible heat fluxes. Figure 11 depicts the heat flux anomalies for DHW, NHW, and CHW. At this point it is also worth clarifying that given the minimal heat fluxes at night, this study focuses on analyzing anomalies in surface latent and sensible heat fluxes during daytime hours. In continental regions such as West Turkey, South Italy, West/Central Greece and Eastern Balkans, here examined types of HWs are typically characterized by higher-than-normal latent heat flux and lower-than-normal sensible heat flux. It is worth mentioning that the observed positive anomalies in soil moisture (Fig. 10d, e, f) appear to contradict the increase in latent flux (Fig. 11a, b, c) during these HWs, over the above areas. This could be attributed to the impact of topographical features of these specific regions and the land use. For instance, in agricultural areas such as in Central Greece and South Italy, the surface soil moisture can remain relatively low if irrigation is applied unevenly or water infiltrates too quickly into the deeper soil layers, while latent heat flux remains high due to evapotranspiration. Additionally, in regions like Western Turkey, low soil moisture but high latent heat flux may arise from the availability of surface water (lakes and rivers) that sustains evaporation despite dry soils. Last but not least, regions dominated by forests, such as North Greece, South and Central Bulgaria are often better able to access deeper water supplies in the soil, maintaining transpiration and latent heat flux, even if the topsoil is dry and thereby rapidly increase sensible fluxes. Apart from these regions, the

spatial patterns of daytime surface latent heat flux align with soil moisture levels during here examined heatwave events. Reduced soil moisture leads to a decrease in surface latent heat flux, indicating that energy dynamics in these areas are predominantly governed by water availability, which primarily influences evapotranspiration.

Moreover, when soil moisture restricts latent heat flux, more energy is allocated to sensible heat, resulting in higher near-surface air temperatures. This phenomenon is closely linked to droughts and HWs. The enhanced transfer of sensible heat from the surface to the atmosphere in most of continental areas raises near-surface temperatures, increasing the occurrence of DHW and CHW (Fig. 11b, f). Compared to DHW and CHW, NHW exhibit less pronounced anomalies in surface sensible heat flux (Fig. 11e), with generally smaller magnitudes. Table S1 summarizes the key atmospheric and surface conditions influencing the examined types of heatwaves in the Eastern Mediterranean, highlighting the distinct physical mechanisms contributing to each type of heatwave.

The observed synoptic patterns associated with various heatwave types in Eastern Mediterranean show similarities to those observed during heatwave events in other parts of the world. For instance, Luo et al. (2022), estimated that DHW are accompanied by increased downward shortwave radiation under a clear sky and dry conditions, whereas NHW are characterized by more cloudy and moist conditions in Southern China. The same patterns have been identified as playing a crucial role in the occurrence of HWs in Europe (Liu et al. 2020a, b), as well as over the contiguous United States (Thomas et al. 2020). Previous research has also identified dynamic processes, such as atmospheric circulation, and land cover as key drivers for the occurrence of HWs. For instance, Harpaz et al. (2014) suggests that extreme summer events over the Eastern Mediterranean are primarily influenced by eastward-traveling mid-latitude disturbances rather than the Asian Monsoon. In addition, land cover influences soil water content by affecting evaporation and plays a key role in regulating surface energy and atmospheric moisture levels (Wang et al. 2024; De Kauwe et al. 2019). Taking the aforementioned results into account, agricultural and rich in water bodies regions, such as South Italy, West/Central Greece, Eastern Balkans, and West Turkey, which experience positive anomalies in soil moisture (Fig. 10), generally associated with higher-than-usual latent heat flux and lower-than-usual sensible heat flux during here examined types of HWs (Fig. 11). This implies that topographical features and land cover significantly influence these anomalies by affecting the availability of water, vegetation, and the energy balance over these regions. However, the spatial distribution of daytime surface latent heat flux consistently corresponds to soil moisture levels during

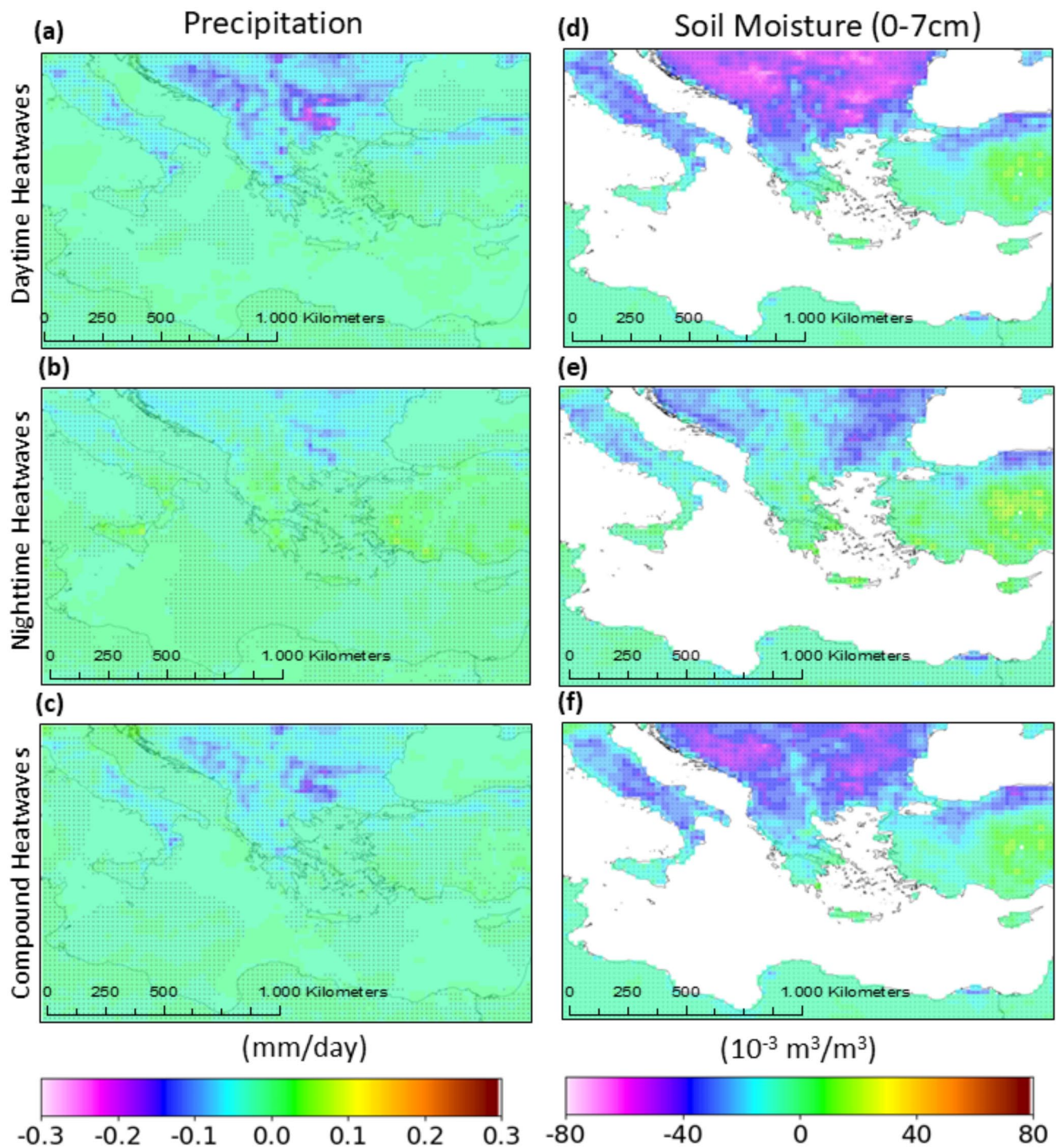


Fig. 10 The daily composite averages of the total precipitation anomalies (left pannel) and soil moisture anomalies (right pannel) for daytime, nighttime, and compound HWs in Eastern Mediterranean. Dots

indicate statistical significance at the 0.05 level, determined using Mann-Kendall test

all heatwave events in other regions. Lower soil moisture results in a reduction of surface latent heat flux, highlighting that energy dynamics are largely driven by water availability, which primarily affects evapotranspiration.

To sum up, these findings indicate a significant increase in the frequency and intensity of heatwaves in the Eastern Mediterranean, with CHW showing the most pronounced trends. The distinct atmospheric and land-atmosphere interactions driving DHW, NHW, and CHW reveal complex

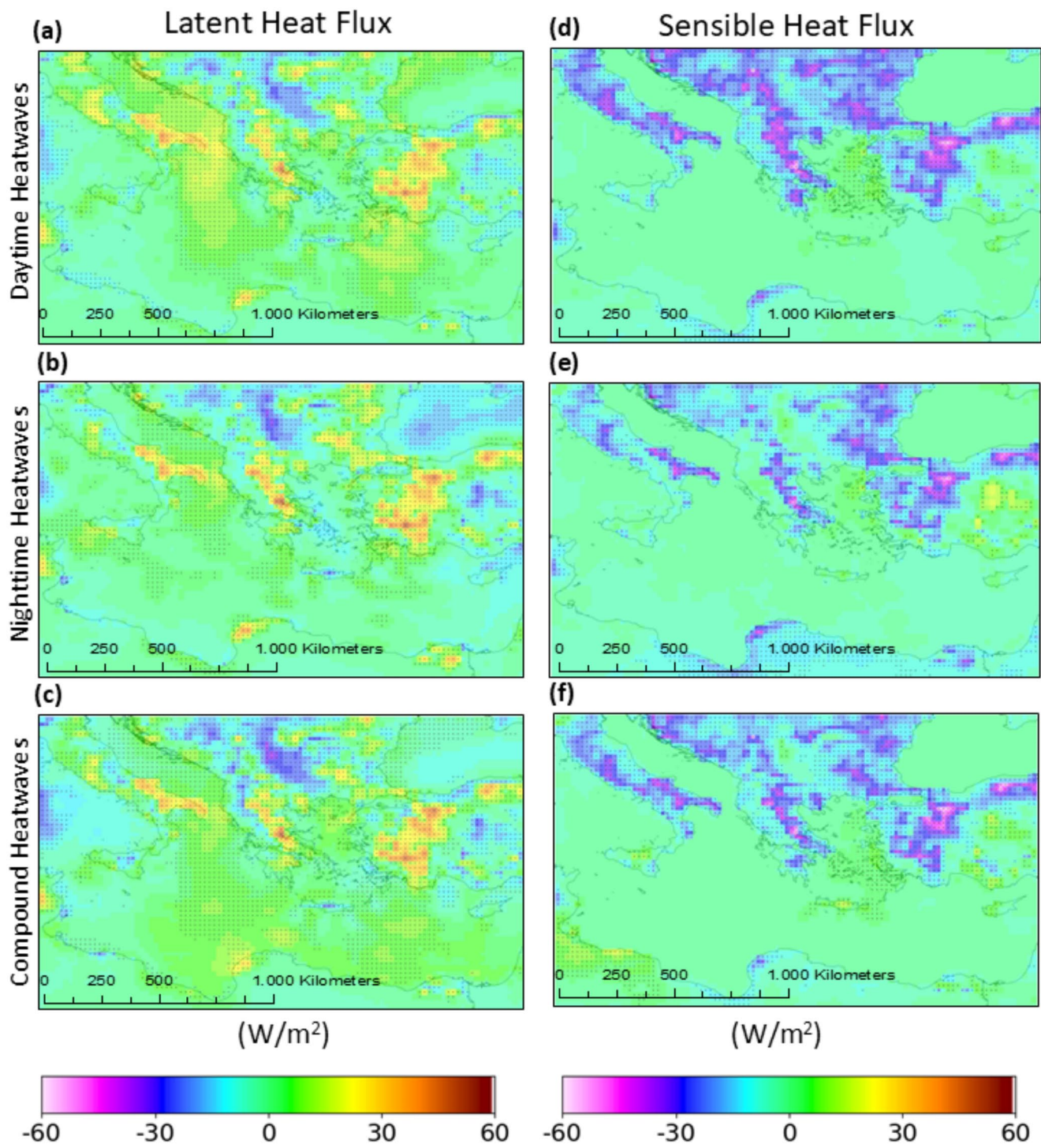


Fig. 11 The daytime composite averages of the surface latent heat flux anomalies (left pannel) and surface sensible heat flux anomalies (right pannel) for daytime, nighttime, and compound HWs in Eastern Medi-

terranean. Dots indicate statistical significance at the 0.05 level, determined using Mann-Kendall test

patterns that require tailored strategies for mitigation and adaptation. Given the critical role of local factors such as topography, land cover, and UHI, adaptation efforts must be region-specific to address the unique challenges presented by each type of heatwave. Furthermore, the intensification

of these extreme heat events underscores the urgent need for comprehensive adaptive strategies. Urban planning should focus on enhancing resilience through the expansion of green infrastructure, such as parks and shaded areas, and the use of reflective building materials to reduce the heat

absorbed by cities. In addition, improving public health infrastructure with early warning systems and dedicated cooling centers is essential to safeguard vulnerable populations during heatwave events. On a broader scale, land-use management strategies that preserve natural vegetation and restore ecosystems are crucial for regulating local climates and buffering the impacts of rising temperatures. By incorporating these measures into long-term adaptation policies, the region can build resilience against future heatwaves, reduce their adverse effects on public health and ecosystems, and strengthen overall climate resilience.

4 Summary and conclusions

This study categorizes heatwave (HW) events in the Eastern Mediterranean during the summer seasons from 1981 to 2023 into three types: compound (CHW), independent daytime (DHW), and independent nighttime heatwaves (NHW). It further investigates the processes and mechanisms driving each type of HW. The findings revealed a significant increase in here examined HW types, with CHW showing the most pronounced rise in frequency and intensity, particularly over the Mediterranean Sea, South Italy, West Turkey, Central Greece, and the Adriatic coast. Notably, NHW frequency has increased at twice the rate of DHW, highlighting the growing prevalence of nighttime heat extremes.

A key takeaway from this study is the diversity of atmospheric mechanisms influencing here examined HW types. DHW and CHW are strongly linked to clear-sky conditions, increased shortwave radiation, and drier environments, while NHW is characterized by higher humidity, increased cloud cover, and enhanced nighttime longwave radiation. These differences highlight land-atmosphere interactions as critical drivers of HW intensity and duration. The increasing occurrence of NHW and CHW suggests an amplified role of anthropogenic climate change, particularly through UHI effects and rising greenhouse gas emissions. The persistence of heat, especially at night, presents serious risks to human health and well-being, as it reduces nighttime cooling and disproportionately affects vulnerable populations.

While this study provides a comprehensive analysis of HW trends and mechanisms, some limitations should be acknowledged. The use of reanalysis datasets may introduce uncertainties, particularly in capturing small-scale urban effects. Additionally, this study does not directly assess future climate projections, which would be valuable for understanding how HW patterns will evolve under different climate scenarios. Further research should focus on high-resolution urban studies to assess how local land cover and infrastructure amplify HWs, as well as on climate model

simulations to project future HW behavior and evaluate mitigation strategies.

Given the increasing frequency and intensity of HWs, urgent adaptation measures are needed to mitigate their impacts on society, ecosystems, and public health. Urban areas, particularly in Mediterranean regions, are highly vulnerable to heatwaves, and as such, more effective planning and management strategies are essential. These strategies should aim at reducing exposure to extreme heat, especially in urban settings where the effects of the UHI are most pronounced. Implementing green infrastructure, such as urban parks, green roofs, and increased tree canopy cover, can help reduce surface temperatures by increasing shade, enhancing evaporative cooling, and improving air quality. Furthermore, the use of reflective and cool materials for roofing, pavements, and road surfaces can help decrease the heat absorption of urban areas during the day. Cool roofs and reflective pavements have been shown to lower surface temperatures, helping to reduce the energy demand for cooling and reducing the urban heat accumulation at night. These materials can complement natural cooling methods such as vegetation by preventing excessive heat retention and by promoting the dissipation of heat into the atmosphere. The adoption of these strategies in cities can significantly reduce both daytime and nighttime heat extremes, providing relief for residents, particularly during prolonged heatwave events. Additionally, enhancing the design and insulation of buildings to improve natural ventilation and reduce the need for energy-intensive air conditioning systems can further mitigate the effects of heatwaves. The integration of passive cooling techniques, such as improved window shading, ventilation strategies, and the use of insulating materials, can reduce indoor temperatures and promote more comfortable living conditions during heat events. Another critical strategy involves improving early warning systems and climate adaptation policies. By incorporating climate projections and real-time heat data, these systems can provide advanced warnings for heatwaves, enabling vulnerable communities to take necessary precautions. Public awareness campaigns and better-targeted health interventions, such as providing cooling centers for the elderly and vulnerable populations, can save lives and alleviate the health impacts of extreme heat.

In conclusion, this study provides a foundation for future research and policy interventions aimed at improving resilience to extreme heat in the Eastern Mediterranean and similar climate-sensitive regions. The findings underscore the importance of adopting comprehensive heatwave mitigation strategies, which should be based on a combination of green infrastructure, reflective materials, building design, and adaptive public health measures. This integrated approach will not only help reduce the immediate impacts

of heatwaves but also contribute to long-term climate adaptation and resilience. Effective mitigation strategies are crucial for minimizing the risks posed by heatwaves and safeguarding both the environment and human health in the face of climate change.

Supplementary Information The online version contains supplementary material available at <https://doi.org/10.1007/s00704-025-05429-8>.

Author contributions Ilias Petrou: Data curation, Methodology, Software, Formal analysis, Writing and editing. Pavlos Kassomenos: Conceptualization, Supervision, Writing – review & editing.

Funding This research did not receive any specific grant from funding agencies in the public, commercial, or not-for-profit sectors.

Data availability No datasets were generated or analysed during the current study.

Code availability Not applicable.

Declarations

Ethical approval Not applicable. This research did not involve any studies with human participants, animals, or sensitive data that required ethics approval.

Consent to participate Not applicable. This study did not involve human participants, animals, or any sensitive data that would require ethical approval.

Consent for publication Not applicable. This research did not involve any human participants

Competing interests The authors declare no competing interests.

References

- Anderson B, Bell M (2011) Heat waves and mortality in new York. *NY Epidemiol* 22(1):S20. <https://doi.org/10.1097/01.ede.0000391719.31370.34>
- Arsad FS, Hod R, Ahmad N, Ismail R, Mohamed N, Baharom M, Osman Y, Radi MFM, Tangang F (2022) The impact of heatwaves on mortality and morbidity and the associated vulnerability factors: A systematic review. *Int J Environ Res Public Health* 19:16356. <https://doi.org/10.3390/ijerph192316356>
- Barbier J, Guichard F, Bouinol D et al (2017) Detection of intra-seasonal large-scale heat waves: characteristics and historical trends during the Sahelian spring. *J Clim* 31:61–80. <https://doi.org/10.1175/JCLI-D-17-0244.1>
- Black E, Blackburn M, Harrison G, Hoskins B, Methven J (2004) Factors contributing to the summer 2003 European heatwave. *Weather* 59:217–223. <https://doi.org/10.1256/wea.74.04>
- Boé J (2013) Modulation of soil moisture-precipitation interactions over France by large scale circulation. *Clim Dyn* 40:875–892. <https://doi.org/10.1007/s00382-012-1380-6>
- Carril AF, Gualdi S, Cherchi A et al (2008) Heatwaves in Europe: areas of homogeneous variability and links with the regional to large-scale atmospheric and SSTs anomalies. *Clim Dyn* 30:77–98. <https://doi.org/10.1007/s00382-007-0274-5>
- Cassou C, Terray L, Phillips AS (2005) Tropical Atlantic influence on European heat waves. *J Clim* 18:2805–2811. <https://doi.org/10.1175/JCLI3506.1>
- Chen Y, Zhai P (2017) Revisiting summertime hot extremes in China during 1961–2015: overlooked compound extremes and significant changes. *Geophys Res Lett* 44:5096–5103. <https://doi.org/10.1002/2016GL072281>
- De Kauwe MG, Medlyn BE, Pitman AJ, Drake JE, Ukkola A, Griebel A, Pendall E, Prober S, Roderick M (2019) Examining the evidence for decoupling between photosynthesis and transpiration during heat extremes. *Biogeosciences* 16:903–916. <https://doi.org/10.5194/bg-16-903-2019>
- Della-Marta PM, Haylock MR, Luterbacher J, Wanner H (2007) Doubled length of Western European summer heat waves since 1880. *J Geophys Res* 112:D15103. <https://doi.org/10.1029/2007JD008510>
- Di Napoli C, Pappenberger F, Cloke H (2018) Assessing heat-related health risk in Europe via the universal thermal climate index (UTCI). *Int J Biometeorol* 62(7):1155–1165. <https://doi.org/10.1007/s00484-018-1518-2>
- Dirmeyer PA, Balsamo G, Blyth EM, Morrison R, Cooper HM (2021) Land-atmosphere interactions exacerbated the drought and heatwave over Northern Europe during summer 2018. *AGU Adv* 2. <https://doi.org/10.1029/2020AV000283>. e2020AV000283
- Dole R, Hoerling M, Perlitz J, Eischeid J, Pegion P, Zhang T, Quan XW, Xu T, Murray D (2011) Was there a basis for anticipating the 2010 Russian heat Wave?? *Geophys Res Lett* 38:L06702. <https://doi.org/10.1029/2010GL046582>
- Dong L, Mitra C, Green S, Burt E (2018) The dynamical linkage of atmospheric blocking to drought, heatwave and urban heat Island in southeastern US: A Multi-Scale case study. *Atmosphere* 9(1):33. <https://doi.org/10.3390/atmos9010033>
- Douville H, Colin J, Krug E, Cattiaux J, Thao S (2016) Midlatitude daily summer temperatures reshaped by soil moisture under climate change. *Geophys Res Lett* 43:812–818. <https://doi.org/10.1002/2015GL06222>
- Engdaw MM, Ballinger AP, Hegerl GC, Steiner AK (2022) Changes in temperature and heat waves over Africa using observational and reanalysis data sets. *Int J Climatol* 42(2):1165–1180. <https://doi.org/10.1002/joc.7295>
- Felsche E, Böhnisch A, Ludwig R (2023) Inter-seasonal connection of typical European heatwave patterns to soil moisture. *Npj Clim Atmos Sci* 6:1. <https://doi.org/10.1038/s41612-023-00330-5>
- Felsche E, Böhnisch A, Poschlod B et al (2024) European hot and dry summers are projected to become more frequent and expand Northwards. *Commun Earth Environ* 5:410. <https://doi.org/10.1038/s43247-024-01575-5>
- Fernandes R, Fragoso M (2021) Assessing heatwaves and their association with North African dust intrusions in the Algarve (Portugal). *Atmosphere* 12(9):1090. <https://doi.org/10.3390/atmos12091090>
- Fischer E, Schär C (2010) Consistent geographical patterns of changes in high-impact European heatwaves. *Nat Geosci* 3:398–403. <https://doi.org/10.1038/ngeo866>
- Founda D, Giannakopoulos C (2009) The exceptionally hot summer of 2007 in Athens, Greece—A typical summer in the future climate?? *Glob Planet Change* 67:227–236. <https://doi.org/10.1016/j.gloplacha.2009.03.013>
- Founda D, Katavoutas G, Pierros F, Mihalopoulos N (2022) The extreme heat wave of summer 2021 in Athens (Greece): cumulative heat and exposure to heat stress. *Sustainability* 14:7766. <https://doi.org/10.3390/su14137766>
- Fransson A, Carlstedt AB, Gustafsson S (2023) Older adults' occupations in heat waves: A scoping review. *Scand J Occup Ther*

- 30(7):1000–1015. <https://doi.org/10.1080/11038128.2023.2231165>
- García-Herrera R, Díaz J, Trigo RM, Luterbacher J, Fischer EM (2010) A review of the European summer heat wave of 2003. *Crit Rev Environ Sci Technol* 40(4):267–306. <https://doi.org/10.1080/10643380802238137>
- Gasparrini A, Armstrong B (2011) The impact of heat waves on mortality. *Epidemiology* 168–73. <https://doi.org/10.1097/EDE.0b013e3181fded99>
- Gilbert RO (1987) Statistical methods for environmental pollution monitoring. Van Nostrand Reinhold, New York
- Guillod B, Orlowsky B, Miralles D et al (2015) Reconciling Spatial and Temporal soil moisture effects on afternoon rainfall. *Nat Commun* 6:6443. <https://doi.org/10.1038/ncomms7443>
- Harpaz T, Ziv B, Saaroni H, Beja E (2014) Extreme summer temperatures in the East Mediterranean—dynamical analysis. *Int J Climatol* 34:849–862. <https://doi.org/10.1002/joc.3727>
- Hirschi M, Seneviratne S, Alexandrov V et al (2011) Observational evidence for soil-moisture impact on hot extremes in southeastern Europe. *Nat Geosci* 4:17–21. <https://doi.org/10.1038/ngeo1032>
- Hoy A, Hänsel S, Maugeri M (2020) An endless summer: 2018 heat episodes in Europe in the context of secular temperature variability and change. *Int J Climatol* 40:6315–6336. <https://doi.org/10.1002/joc.6582>
- Ionita M, Caldarescu DE, Nagavciuc V (2021) Compound hot and dry events in Europe: variability and Large-Scale drivers. *Front Clim* 3:688991. <https://doi.org/10.3389/fclim.2021.688991>
- Ji L, Chen H (2024) Differences in variations of Long-Lived and Short-Lived summer heat waves during 1981–2020 over Eastern China and their corresponding Large-Scale circulation anomalies. *J Meteorol Res* 38:414–436. <https://doi.org/10.1007/s13351-024-3162-6>
- Lazoglu G, Hadjinicolaou P, Sofokleous I, Bruggeman A, Zittis G (2024) Climate change and extremes in the mediterranean Island of Cyprus: from historical trends to future projections. *Environ Res Commun* 6095020. <https://doi.org/10.1088/2515-7620/ad7927>
- Lemus-Canovas M, Gonzalez-Herrero S, Trapero L, Albalat A, Insua-Costa D, Senande-Rivera M, Miguez-Macho (2023) Attributing heatwaves to climate change in mountainous areas. An analysis of the summer 2022 heatwaves in the Pyrenees, EGU General Assembly 2023, Vienna, Austria, 23–28 Apr 2023, EGU23-11234. <https://doi.org/10.5194/egusphere-egu23-11234>
- Lemus-Canovas M, Insua-Costa D, Trigo RM, Miralles DG (2024) Tracing the impact of drought on the Western Mediterranean's record-shattering Spring 2023 heatwave, EMS Annual Meeting 2024, Barcelona, Spain, 1–6 Sep 2024, EMS2024-1010 <https://doi.org/10.5194/ems2024-1010>
- Li Y, Ding Y, Li W (2017) Observed trends in various aspects of compound heat waves across China from 1961 to 2015. *J Meteorol Res* 31:455–467. <https://doi.org/10.1007/s13351-017-6150-2>
- Liu L, Gudmundsson L, Hauser M et al (2020a) Soil moisture dominates dryness stress on ecosystem production globally. *Nat Commun* 11:4892. <https://doi.org/10.1038/s41467-020-18631-1>
- Liu X, He B, Guo L, Huang L, Chen D (2020b) Similarities and differences in the mechanisms causing the European summer heatwaves in 2003, 2010, and 2018. *Earth's Future*, 7, e2019EF001386. <https://doi.org/10.1029/2019EF001386>
- Liu J, Qi J, Yin P et al (2024) Rising cause-specific mortality risk and burden of compound heatwaves amid climate change. *Nat Clim Chang* 14:1201–1209. <https://doi.org/10.1038/s41558-024-02137-5>
- Lopes A, Alves E, Alcoforado M, Machete R (2013) Lisbon urban heat island updated: New highlights about the relationships between thermal patterns and wind regimes. *Advances in Meteorology*, 2013, 1–11. <https://doi.org/10.1155/2013/487695>
- Luo M, Lau NC, Liu Z (2022) Different mechanisms for daytime, nighttime, and compound heatwaves in Southern China. *Weather Clim Extremes* 36:100449. <https://doi.org/10.1016/j.wace.2022.100449>
- Majeed H, Floras JS (2022) Warmer summer nocturnal surface air temperatures and cardiovascular disease death risk: a population-based study. *BMJ Open* 12:e056806. <https://doi.org/10.1136/bmopen-2021-056806>
- Meehl GA, Tebaldi C (2004) More intense, more frequent, and longer lasting heat waves in the 21st century. *Science* 31305(5686):994–7. <https://doi.org/10.1126/science.1098704>
- Nairn JR, Fawcett RJB (2015) The excess heat factor: A metric for heatwave intensity and its use in classifying heatwave severity. *Int J Environ Res Public Health* 12(1):227–253. <https://doi.org/10.3390/ijerph12010027>
- Oliveira A, Lopes A, Correia E, Niza S, Soares A (2021) Heatwaves and summer urban heat Islands: A daily cycle approach to unveil the urban thermal signal changes in Lisbon, Portugal. *Atmos* 12(3):1–23. <https://doi.org/10.3390/atmos12030292>
- Oliveira A, Lopes A, Soares A (2022) Excess heat factor climatology, trends, and exposure across European functional urban areas. *Weather Clim Extremes* 36(100455):1–12. <https://doi.org/10.1016/j.wace.2022.100455>
- Pardo SK, Paredes-Fortuny L (2024) Uneven evolution of regional European summer heatwaves under climate change. *Weather Clim Extremes* 43:100648. <https://doi.org/10.1016/j.wace.2024.100648>
- Pastor F, Paredes-Fortuny L, Khodayar S (2024) Mediterranean marine heatwaves intensify in the presence of concurrent atmospheric heatwaves. *Commun Earth Environ* 5:797. <https://doi.org/10.1038/s43247-024-01982-8>
- Peel MC, Finlayson BL, McMahon TA (2007) Updated world map of the Köppen-Geiger climate classification. *Hydroclim Earth Syst Sci* 11:1633–1644. <https://doi.org/10.5194/hess-11-1633-2007>
- Perkins SE, Alexander VL (2013) On the measurement of heat waves. *J Clim* 26:4500–4517. <https://doi.org/10.1175/JCLI-D-12-00383.1>
- Perkins SE, Alexander LV, Nairn JR (2012) Increasing frequency, intensity and duration of observed global heatwaves and warm spells. *Geophys Res Lett* 39:L20714. <https://doi.org/10.1029/2012GL053361>
- Purich A, Cowan T, Cai W, van Rensch P, Uotila P, Pezza A, Boschat G, Perkins S (2014) Atmospheric and oceanic conditions associated with Southern Australian heat waves: A CMIP5 analysis. *J Clim* 27:7807–7829. <https://doi.org/10.1175/JCLI-D-14-00098.1>
- Ridder NN, Pitman AJ, Ukkola AM (2021) Do CMIP6 climate models simulate global or regional compound events skillfully? *Geophys Res Lett* 48. <https://doi.org/10.1029/2020GL091152.,e2020GL091152>
- Rouges E, Ferranti L, Kantz H, Pappenberger F (2023) European heatwaves: link to large-scale circulation patterns and intraseasonal drivers. *Int J Climatol* 43(7):3189–3209. <https://doi.org/10.1002/joc.8024>
- Rousi E, Kornhuber K, Beobide-Arsuaga G et al (2022) Accelerated Western European heatwave trends linked to more-persistent double jets over Eurasia. *Nat Commun* 13:3851. <https://doi.org/10.1038/s41467-022-31432-y>
- Russo S, Dosio A, Graversen RG, Sillmann J, Carrao H, Dunbar MB, Singleton A, Montagna P, Barbola P, Vogt JV (2014) Magnitude of extreme heat waves in present climate and their projection in a warming world. *J Geophys Res Atmos* 119(500–12,512). <https://doi.org/10.1002/2014JD022098>
- Russo S, Sillmann J, Fischer EM (2015) Top ten European heatwaves since 1950 and their occurrence in the coming decades. *Environ Res Lett* 10:124003. <https://doi.org/10.1088/1748-9326/10/12/124003>

- Schoetter R, Cattiaux J, Douville H (2015) Changes of Western European heat wave characteristics projected by the CMIP5 ensemble. *Clim Dyn* 45:1601–1616. <https://doi.org/10.1007/s00382-014-2434-8>
- Serra C, Lana X, Martínez MD et al (2024) Summer heatwaves trends and hotspots in the Barcelona metropolitan region (1914–2020). *Theor Appl Climatol* 155:4681–4702. <https://doi.org/10.1007/s0704-024-04912-y>
- Stéfanon M, Drobinski P, D'Andrea F, Lebeaupin-Brossier C, Bastin S (2014) Soil moisture-temperature feedbacks at meso-scale during summer heat waves over Western Europe. *Clim Dyn* 42:1309–1324. <https://doi.org/10.1007/s00382-013-1794-9>
- Su Q, Dong B (2019) Recent decadal changes in heat waves over China: drivers and mechanisms. *J Clim* 32:4215–4234. <https://doi.org/10.1175/JCLI-D-18-0479.1>
- Sutanto SJ, Vitolo C, Di Napoli C, D'Andrea M, Van Lanen HAJ (2020) Heatwaves, droughts, and fires: exploring compound and cascading dry hazards at the pan-European scale. *Environ Int* 134:105276. <https://doi.org/10.1016/j.envint.2019.105276>
- Taylor CM (2015) Detecting soil moisture impacts on convective initiation in Europe. *Geophys Res Lett* 42:4631–4638. <https://doi.org/10.1002/2015GL064030>
- Thomas NP, Bosilovich MG, Marquardt Collow AB, Koster RD, Schubert SD, Dezfuli A, Mahanama SP (2020) Mechanisms associated with daytime and nighttime heat waves over the contiguous United States. *J Appl Meteor Climatol* 59:1865–1882. <https://doi.org/10.1175/JAMC-D-20-0053.1>
- Tripathy KP, Mishra AK (2023) How unusual is the 2022 European compound drought and heatwave event? *Geophys Res Lett* 50. <https://doi.org/10.1029/2023GL105453> e2023GL105453
- Ullah S, You Q, Ullah W, Ali A, Xie W, Xie X (2019) Observed changes in temperature extremes over China–Pakistan economic corridor during 1980–2016. *Int J Climatol* 39:1457–1475. <https://doi.org/10.1002/joc.5894>
- van Heerwaarden CC, Teuling AJ (2014) Disentangling the response of forest and grassland energy exchange to heatwaves under idealized land–atmosphere coupling. *Biogeosciences* 11:6159–6171. <https://doi.org/10.5194/bg-11-6159-2014>
- Vautard R, Yiou P, D'Andrea F, de Noblet N, Viovy N, Cassou C, Polcher J, Ciais P, Kageyama M, Fan Y (2007) Summertime European heat and drought waves induced by wintertime Mediterranean rainfall deficit. *Geophys Res Lett* 34:L07711. <https://doi.org/10.1029/2006GL028001>
- Vautard R, Gobiet A, Jacob D et al (2013) The simulation of European heat waves from an ensemble of regional climate models within the EURO-CORDEX project. *Clim Dyn* 41:2555–2575. <https://doi.org/10.1007/s00382-013-1714-z>
- Vogel MM, Orth R, Cheruy F, Hagemann S, Lorenz R, van den Hurk BJM, Seneviratne SI (2017) Regional amplification of projected changes in extreme temperatures strongly controlled by soil moisture-temperature feedbacks. *Geophys Res Lett* 44:1511–1519. <https://doi.org/10.1002/2016GL071235>
- Wang J, Chen Y, Tett SFB et al (2020a) Anthropogenically-driven increases in the risks of summertime compound hot extremes. *Nat Commun* 11:528. <https://doi.org/10.1038/s41467-019-14233-8>
- Wang J, Feng J, Yan Z, Chen Y (2020b) Future risks of unprecedented compound heat waves over three vast urban agglomerations in China. *Earth's Future* 8. <https://doi.org/10.1029/2020EF001716> e2020EF001716
- Wang C, Li Z, Chen Y, Li Y, Ouyang L, Zhu J et al (2024) Changes in global heatwave risk and its drivers over one century. *Earth's Future* 12:e2024EF004430. <https://doi.org/10.1029/2024EF004430>
- Wehrli K, Guillod BP, Hauser M, Leclair M, Seneviratne SI (2019) Identifying key driving processes of major recent heat waves. *J Geophys Research: Atmos* 124:11746–11765. <https://doi.org/10.1029/2019JD030635>
- Wei J, Dirmeyer PA (2012) Dissecting soil moisture-precipitation coupling. *Geophys Res Lett* 39:L19711. <https://doi.org/10.1029/2012GL053038>
- Wu S, Luo M, Zhao R et al (2023) Local mechanisms for global daytime, nighttime, and compound heatwaves. *Npj Clim Atmos Sci* 6:36. <https://doi.org/10.1038/s41612-023-00365-8>
- Yang Y, Liu C, Ou N, Liao X, Cao N, Chen N, Jin L, Zheng R, Yang K, Su Q (2022) Moisture transport and contribution to the continental precipitation. *Atmosphere* 13(10):1694. <https://doi.org/10.3390/atmos13101694>
- Zittis G, Hadjinicolaou P, Fnais M et al (2016) Projected changes in heat wave characteristics in the Eastern Mediterranean and the middle East. *Reg Environ Change* 16:1863–1876. <https://doi.org/10.1007/s10113-014-0753-2>
- Zscheischler J, Martius O, Westra S et al (2020) A typology of compound weather and climate events. *Nat Rev Earth Environ* 1:333–347. <https://doi.org/10.1038/s43017-020-0060-z>
- Zuo J, Pullen S, Palmer J, Bennetts H, Chileshe N, Ma T (2015) Impacts of heat waves and corresponding measures: a review. *J Clean Prod* 92:1–12. <https://doi.org/10.1016/j.jclepro.2014.12.007>

Publisher's note Springer Nature remains neutral with regard to jurisdictional claims in published maps and institutional affiliations.

Springer Nature or its licensor (e.g. a society or other partner) holds exclusive rights to this article under a publishing agreement with the author(s) or other rightsholder(s); author self-archiving of the accepted manuscript version of this article is solely governed by the terms of such publishing agreement and applicable law.